2009-09-03

Spectroscopic Investigation of the Anatase-to-Rutile Transformation of Sol-Gel Synthesised TiO2 Photocatalysts

Nicholas Nolan
Technological University Dublin, nicholas.nolan@tudublin.ie

Suresh Pillai
Technological University Dublin, suresh.pillai@tudublin.ie

Michael Seery
Technological University Dublin, michael.seery@tudublin.ie

Recommended Citation

Nolan, N., Pillai, S., Seery, M. (2009): Spectroscopic Investigation of the Anatase-to-Rutile Transformation of Sol-Gel Synthesised TiO2 Photocatalysts. *Journal of Physical Chemistry C*, 113, 2009, pp. 16151-16157. doi:10.1021/jp904358g

Funder: Environmental Protection Agency, Ireland

ohio2/yjy-yjy/yjy-yjy/yjy99907/yjy9845d07z | xppws | 23:ver.3 | 8/6/09 | 18:56 | Msc: jp-2009-04358g | TEID: mrh00 | BATID: 00000

Spectroscopic Investigation of the Anatase-to-Rutile Transformation of Sol−Gel-Synthesized TiO_2 Photocatalysts

Nicholas T. Nolan,[†,‡] Michael K. Seery,*[,†] and Suresh C. Pillai[‡]

School of Chemical and Pharmaceutical Sciences, Dublin Institute of Technology, Kevin Street, Dublin 8, Ireland, and Centre for Research in Engineering Surface Technology (CREST), Focas Institute, Dublin Institute of Technology, Kevin Street, Dublin 8, Ireland

Received: May 11, 2009; Revised Manuscript Received: July 26, 2009

Among the three major phases in titania, anatase is reported to be a better photocatalytically active phase. Anatase to rutile transformations, under normal conditions, usually occurs at a temperatue range of 600−700 °C. Various chemical additives have previously been employed to extend the anatase transition to higher temperatures. The effect of employing various concentrations of formic acid and water on phase transition has systematically been studied by XRD, FTIR, and Raman spectroscopy. A considerably higher anatase phase (41%) has been obtained at 800 °C, and 10% anatase composition is retained after annealing the materials at 900 °C for the optimized composition. On comparison, a control sample which has been prepared without formic acid showed that the rutile phase formed at a temperature of 600 °C, FTIR and Raman studies indicated that the formate group favored a bridging (syn−anti or syn−syn) mode of chelation depending on the reaction conditions. It has been concluded that the resulting syn−anti binding hinders cross-linking of the gel network, resulting in a weakened structure and thus causing the anatase to rutile transformation temperature to occur at a lower temperature than with the syn−syn mode of binding where more ordered gel networks are formed.

Introduction

Titanium dioxide (TiO_2) is a semiconductor metal oxide that attracts much interest due to its wide range of applications which include photovoltaic cells, gas sensors, pigments, and photocatalysis.[1−7] It exists as three different polymorphs: rutile (tetragonal), anatase (tetragonal), and brookite (orthorhombic).[8,9] Rutile is thermodynamically stable, while anatase and brookite are metastable, transforming to rutile under calcination, typically 600−700 °C.[8] Anatase is usually considered to be the most photoactive of the three polymorphs for the degradation of organic pollutants.[10−12]

Anatase-to-rutile phase transformation in TiO_2 is an area of both scientific and technological interest.[6,13] The anatase-to-rutile transformation (ART) is kinetically defined, and the reaction rate is determined by parameters such as particle shape/size,[14] purity,[15] source effects,[16] atmosphere,[17] and reaction conditions.[18] It is agreed that the mechanism for phase transformation of titania is one of nucleation and growth.[19,20] Anatase nanocrystals coarsen, grow, and then transform to rutile only when a critical size is reached.[21] Therefore, phase transformation is dominated by effects such as defect concentration,[22] grain boundary concentration,[23] and particle packing.[24]

Sol−gel synthesis of TiO_2 is regarded as a relatively straightforward synthesis technique and is thus of great interest and use to researchers.[25] Titanium alkoxides are readily hydrolyzed by water due to their susceptibility to nucleophilic attack.[26] Rates of hydrolysis and condensation may be controlled by using organic chelating agents such as acetyl acetone,[27] alkanolamines,[28] diols,[29] and acetic acid[30] to replace alkoxide groups on the central metal atom. This stability improves control over the reaction conditions.[31] Suresh et al. concluded that the pH of the precursor influences the chelation effect of acetic acid and that the extent of chelation of the acetate group decreases with an increase in pH causing weakened gel structures resulting in decreased ART temperatures.[6]

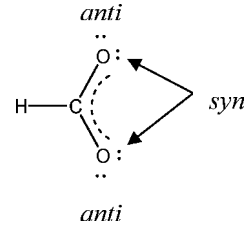

Figure 1. Carboxylate functional group.

FTIR and Raman spectroscopy can be used to determine the binding mode of the carboxylate group. The frequency of the asymmetric carboxylate vibration in the IR spectra, $\upsilon_{as}(COO^-)$, and the magnitude of the separation between the carboxylate stretches, $\Delta = \upsilon_{as}(COO^-) - \upsilon_s(COO^-)$, are often used to determine the mode of the carboxylate binding.[32] In the bridging coordination, one divalent metal cation is bound to one of the oxygen atoms of the COO^- group and another divalent metal cation to the other oxygen, the asymmetric stretch is located at the same position as that of the ionic group.[32,34] The range 200−210 cm^{-1} was derived for ionic formates, and in general, the comparison of the Δ value of the respective complex with the Δ value of the sodium salt should be used for the assignment following the guidelines: (i) bidentate chelating coordination, $\Delta(COO^-)_{\text{formate complex}} \ll \Delta(COO^-)_{\text{sodium salt}}$; (ii) bidentate bridging carboxylate, $\Delta(COO^-)_{\text{formate complex}} \leq \Delta(COO^-)_{\text{sodium salt}}$; (iii) monodentate coordination, $\Delta(COO^-)_{\text{formate complex}} \gg \Delta(COO^-)_{\text{sodium salt}}$.[32,33,35−38]

The carboxylate functional group (Figure 1) has four lone pairs of electrons available for coordination to a metal. These

* To whom correspondence should be addressed. E-mail: michael.seery@dit.ie.
† School of Chemical and Pharmaceutical Sciences.
‡ CREST.

10.1021/jp904358g CCC: $40.75

lone pairs subtend to an angle of 120° and are referred to as the syn and anti lone pairs. On the basis of stereoelectronic arguments, it has been suggested that the syn lone pairs are more basic than those in the anti position.[39]

Previous work studying ART temperatures has been carried out grouping our laboratories where acetic acid was chelated to the titanium alkoxide precursor.[40] It is widely accepted that acetic acid forms a bridging complex to titanium alkoxides.[25,41,42] Titanium dioxide sol−gel materials synthesized using titania alkoxides (without chemical additives) typically transform from anatase to rutile at ~600 °C. However, to the best of the authors' knowledge, no systematic spectroscopy studies have been carried out to investigate titania carboxylate complexes and how different modes of binding affect the ART temperature. In order to determine whether varying ratios of a chelating species alters the ART temperature, the simplest carboxylic acid—formic acid—and titanium isopropoxide in various ratios were used to synthesize a wide range of TiO_2 powders. The formate carboxylate group was chosen because of its versatile coordination behavior.[32] The carboxylate coordinations include ionic, monodentate, bidentate chelating, and bridging.[32] From FTIR and Raman spectroscopy, the role of the chelating agent in the synthesis was examined. Ivanda et al. carried out spectroscopic studies on powders synthesized from an esterfication reaction to find bridging of various carboxylates. However, the paper focused mainly on particle size as opposed to relating oligomeric structure and ART temperatures.[43]

These are practical, efficient, and useful techniques for gaining information on modes of binding. In order to understand why anatase transforms to rutile at different temperatures, these spectroscopic techniques were employed to investigate how the formate group binds to the titanium. Anatase and rutile percentages and transformation temperatures were examined using XRD. It should also be noted that syn−syn, syn−anti bidentate bridging complexes have not been systematically investigated with relation to ART temperatures.

Experimental Section

Titanium tetraisopropoxide (TTIP) was added to formic acid under stirring, resulting in a vigorous exothermic reaction producing a powdered suspension. To the resulting suspension water was added in varying ratios to give total volumes in the range of 10−50 mL. The molar ratios were varied throughout the experiment: TTIP/formic acid remains constant, 1:2, while the water ratio increases 4, 8, 10, 40, 80, and 100. These samples were labeled F_2W_4, F_2W_8, F_2W_{10}, F_2W_{40}, F_2W_{80}, and F_2W_{100}. Similarly, a further 12 samples were prepared where the TTIP/formic acid ratio was increased to 1:4 and 1:10, respectively, the water ratio was increased to replicate samples F_2W_4−F_2W_{100}. The samples were labeled F_4W_4, F_4W_8, F_4W_{10}, F_4W_{40}, F_4W_{80}, and F_4W_{100} when the TTIP/formic acid ratio was 1:4 and for the TTIP/formic acid ratio of 1:10 the samples were labeled $F_{10}W_4$, $F_{10}W_8$, $F_{10}W_{10}$, $F_{10}W_{40}$, $F_{10}W_{80}$, and $F_{10}W_{100}$. $F_{control}$ was synthesized without formic acid to compare the chelating effects of the carboxylate group. After the addition of water, a precipitate was formed which was then filtered, washed with deionized water, and dried at 100 °C for 10 h. Each powder was then calcined at temperatures ranging from 300−1000 °C. XRD patterns of the calcined powders were obtained with a Siemens D500 X-ray powder diffractometer in the diffraction angle range $2\Theta = 20-80°$ using Cu Kα radiation. Anatase/rutile percentages were calculated from the resulting diffractograms using the Spurr equation:[44]

$$\%_{\text{Rutile}} = \frac{1}{1 + 0.8[I_A(101)/I_R(110)]} \quad (1)$$

Where I_A is the intensity of (101) peak and I_R is the intensity of (110) peak.

Infrared and Raman spectroscopy were employed to determine carboxylate binding modes on each powder before or xerogel calcination.

All infrared spectra were obtained on a Perkin-Elmer GX FT-IR and recorded as a KBr disk (1:10 sample/KBr). An ISA Labram was used to record Raman spectra of the powdered samples with an argon ion laser (514.5 nm) as excitation source.

FESEM images were obtained from a Hitachi SU-70 at an operating voltage of 5.0 kV.

Methylene blue is an accepted model organic pollutant for photocatalytic degradation studies and is used as an industrial standard (Japanese standard, JIS R 1703-2:2007); as such, it was used to demonstrate the photocatalytic efficiency of the synthesized TiO_2 powders. Rhodamine 6G (5×10^{-6} M) was used for the comparison of results. In a typical experiment, crystalline TiO_2 (60 mg) was added to methylene blue solution (50 mL, 1×10^{-5} M) and placed in a Q-sun solar simulator[45] with continuous stirring, 5 mL aliquots were withdrawn at timed intervals and the visible absorption spectrum was measured using a Perkin-Elmer Lambda 900 UV−vis spectrometer.

Results and Discussion

In order to investigate the influence of chelation on ART, the effect of various concentrations of water and formic acid on the titania precursor were investigated.

Effect of Water. ***X-ray Diffraction.*** XRD was employed to determine the phase analysis of each powder calcined at increasing temperatures. The percentage of anatase in the calcined sample is shown in Figure 2. All samples were 100% anatase at temperatures 300−500 °C. From Figure 2 it is apparent that for each series of powders (F_2W_4−F_2W_{100}, F_4W_4−F_4W_{100}, and $F_{10}W_4$−$F_{10}W_{100}$), where the TTIP/FA ratio remains constant, that the increase in water promotes the formation of rutile. For the powders F_2W_4−F_2W_{100}, F_2W_4 has the lowest water ratio and it is the only powder with anatase at 700 °C, but the remaining powders have all underwent complete phase transformation to a more thermodynamically stable rutile.

The formic acid ratio was increased for powders F_4W_4−F_4W_{100}, causing improved chelation. This is reflected throughout the six powders, as most retain anatase at 700 °C. Anatase is predominant for F_4W_4 at 700 °C (86%), but the increase in water along the series causes increased rutile formation for the remaining powders. At 800 °C anatase is still dominant for the powder F_4W_4 (61%) and is even present in F_4W_8 (5%); however, the other powders in the series are rutile.

From these results it is clear that an increase in the amount of water used for hydrolysis has an adverse effect on ART temperatures, resulting in the lowering of the ART. This increase in water reduces the acidity of the sol resulting in a decrease in the chelation effect of the formate group.[26,41,42,46] This decrease in chelation results in a weakened gel network and consequently a lowering of ART temperature was observed.[47] Sahni et al. reported that increasing water content causes increased hydrolysis which results in the formation of larger particles that thermodynamically favor phase transformation to rutile.[48]

For powders $F_{10}W_4$−$F_{10}W_{100}$, the sample with the lowest water ratio, $F_{10}W_4$, is one of only two samples where anatase is present at 800 °C. The other is $F_{10}W_{40}$, and the reason why

ohio2/yjy-yjy/yjy-yjy/yjy99907/yjy9845d07z | xppws | 23:ver.3 | 8/6/09 | 18:56 | Msc: jp-2009-04358g | TEID: mrh00 | BATID: 00000

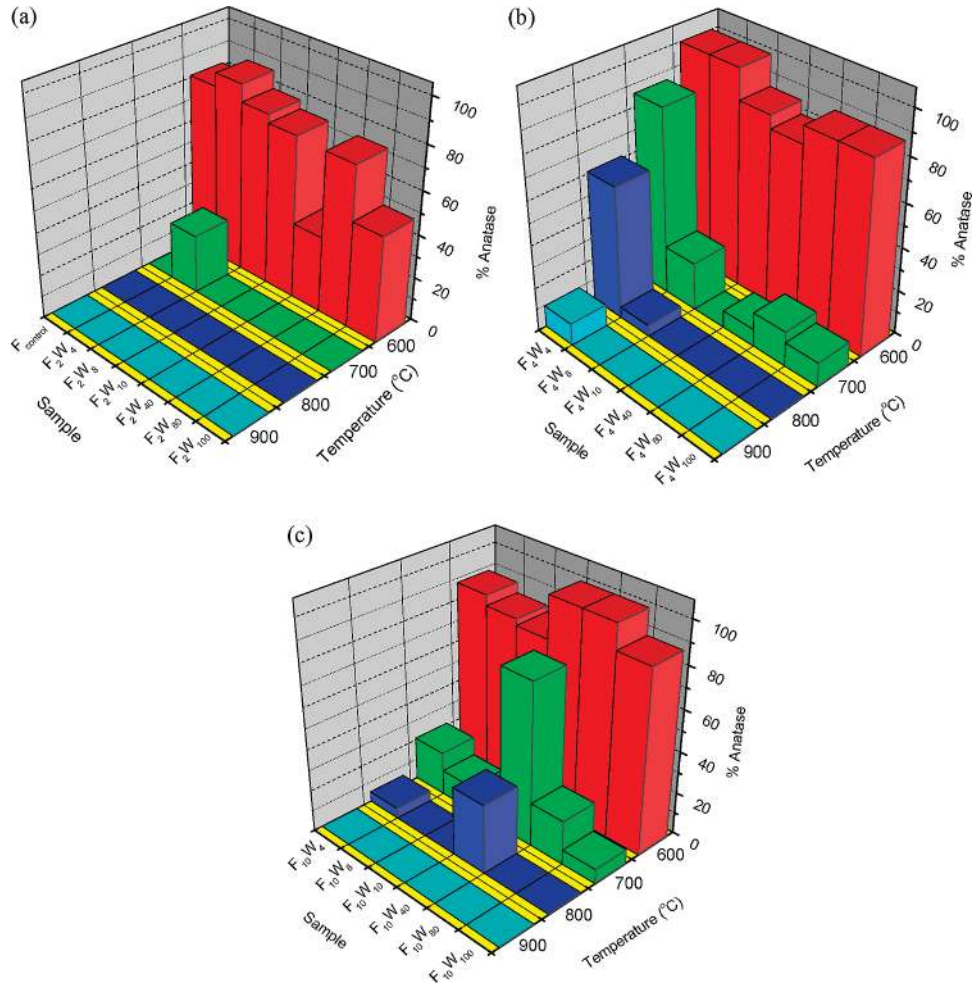

Figure 2. Percentage of anatase in the calcined TiO_2 samples, determined by XRD for materials heated to different temperatures (a) F_2W_4−F_2W_{100}, (b) F_4W_4−F_4W_{100}, and (c) $F_{10}W_4$−$F_{10}W_{100}$.

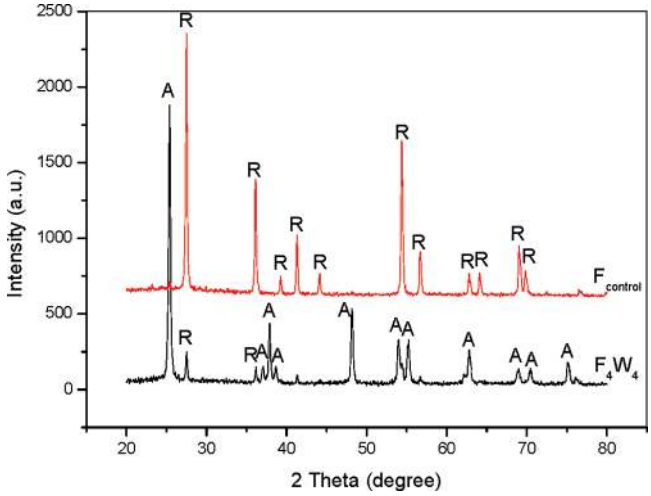

Figure 3. XRD of $F_{control}$ and F_4W_4 at 700 °C. A, anatase; R, rutile.

anatase is present in $F_{10}W_{40}$ is unclear as it has an increased amount of water, whereas powders $F_{10}W_8$, $F_{10}W_{10}$, $F_{10}W_{80}$, and $F_{10}W_{100}$ follow the theory that increased amounts of water cause a reduction in ART temperatures.

From Figure 2, F_4W_4 was found to maintain anatase at temperatures as high as 900 °C. All powders synthesized (bar $F_{10}W_{40}$) showed that as water ratio is increased rutile forms at lower temperatures.

As the carboxylate group may coordinate to Ti in a number of different arrangements[26,32,33,41,42,46] spectroscopic (Raman and IR) studies were carried out on all precalcined samples in order to determine if an increase in water influences the way that the carboxylate group binds to Ti, which in turn affects the anatase to rutile transformation temperature. The morphology of the calcined powders were analyzed using FESEM microscopy and were found to be highly aggregated with an average size of 100−150 nm (Supporting Information 1).

Infrared Spectroscopy. Figure 4 shows the IR spectra of powdered samples F_2W_4 and F_2W_8 (F_2W_8−F_2W_{100} give near identical spectra). At ∼450 cm^{-1} there is a broad peak due to the formation of Ti−O bonds. Peaks at 1350 and 1550 cm^{-1} represent $\nu(COO^-)_{sym}$ and $\nu(COO^-)_{asym}$, respectively. Zalenak et al. determined the mode of bonding of the carboxylate group to the metal atom by calculating Δ, where $\Delta = \nu_{as}(COO^-) - \nu_s(COO^-)$.[32] From the spectra obtained for F_2W_4 and F_2W_8 (Figure 4), Δ = ∼200 cm^{-1}. This value is consistent with the literature value for ionic formate ($HCOO^-$) = ∼201 cm^{-1}.[33]

As has been reported elsewhere, the bidentate bridging carboxylate exists when $\Delta(COO^-)_{formate\ complex} \leq \Delta(COO^-)_{sodium\ salt}$.[33,35−38] Therefore, it is proposed that the formate group binds to the Ti center in bidentate bridging mode such as syn−syn or syn−anti (Figure 5).

It has been reported that metal alkoxo-acetates are formed by the reaction of acetic acid (AcOH) with metal alkoxide,

ohio2/yjy-yjy/yjy-yjy/yjy99907/yjy9845d07z | xppws | 23:ver.3 | 8/6/09 | 18:56 | Msc: jp-2009-04358g | TEID: mrh00 | BATID: 00000

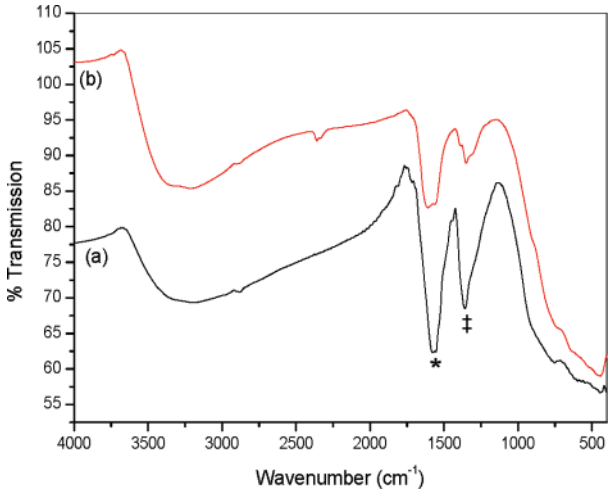

Figure 4. IR spectra of TiO_2 precursor powders (a) F_2W_4 and (b) F_2W_8, where * = $\upsilon_{asym}(COO^-)$ and ‡ = $\upsilon_{sym}(COO^-)$.

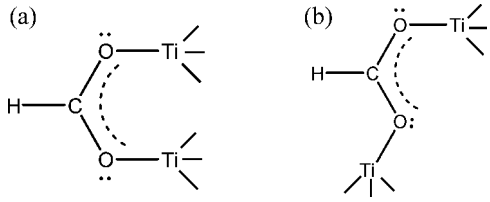

Figure 5. Bidentate bridging modes of the formate group and TTIP (a) syn−syn and (b) syn−anti.

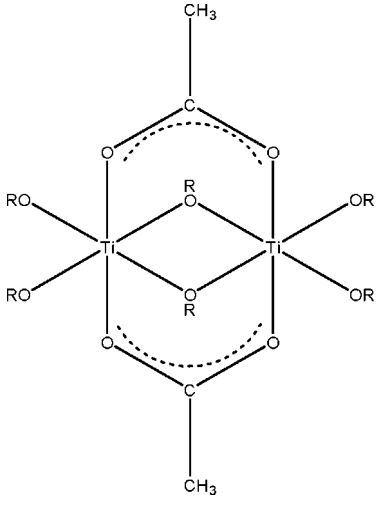

Figure 6. Bridging acetate ligands attached to TTIP.

in which OPr^i (OR) groups on the central titanium atom are preferentially hydrolyzed, whereas bridging acetate ligands remain bonded to titanium throughout much of the condensation process (Figure 6).[25,42]

Since the bridging acetate ligands are not hydrolyzed, the chelated ligands effectively alter the condensation pathway toward promoting the formation of linear polymers composed of edge-sharing octahedra.[42,49] The addition of excess water destabilizes the system by altering the highly cross-linked network structure. The gel having polymeric chains with little branching and cross-linking, as well as a smaller void region, are structurally weak and thus collapse rapidly on calcination forming rutile at lower temperatures.[47]

This can clearly be seen from both the rutile percentage results (Figure 2) and also from the IR spectra (Figure 7) where bands corresponding to the chelated formate group become weaker.

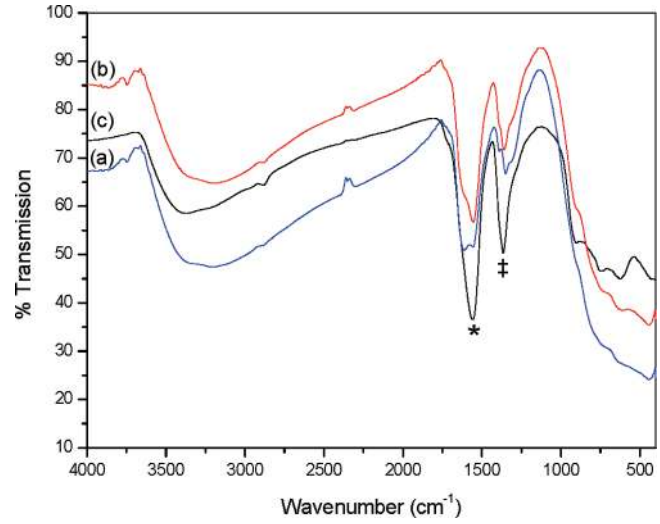

Figure 7. IR spectra of TiO_2 precursor powders (a) F_4W_4, (b) F_4W_8, and (c) F_4W_{10}, where * = $\upsilon_{asym}(COO^-)$ and ‡ = $\upsilon_{sym}(COO^-)$.

From the IR spectra of samples F_4W_4−F_4W_{10} (Figure 7), it can be seen that there is a strong OH peak at ∼2800−3500 cm^{-1}. As the ratio of water is increased in each series (F_2W_4−F_2W_{100}, F_4W_4−F_4W_{100}, $F_{10}W_4$−$F_{10}W_{100}$) it can be seen that the intensity of both $\upsilon_{sym}(COO)$ and $\upsilon_{asym}(COO)$ decrease in relation to both the Ti−O and the OH peaks. F_4W_4 shows the strongest COO stretches and the weakest Ti−O and OH signal when compared with the other samples. It is believed that this is due to an increase in the molar ratio of water which alters the pH of the system as well as increasing hydrolysis and weakening the gel network.[6] This, as has been reported previously, weakens the chelation of the carboxylate group, which will cause weakened COO stretches, facilitating increased hydrolysis, therefore increasing OH stretches and causing a reduction in the anatase to rutile transformation temperature.[6,47,48]

It can also be seen from the IR spectra (Figures 4 and 7) that for samples F_2W_8 and F_4W_{10} two asymmetric (1600 and 1550 cm^{-1}) and two symmetric (1382 and 1340 cm^{-1}) carboxylate stretches were observed. For sample F_4W_4 one asymmetric (1550 cm^{-1}) and one symmetric (1362 cm^{-1}) carboxylate stretch were observed in the IR spectra. The spectra of sample F_4W_8 showed that secondary asymmetric and symmetric stretches were beginning to form. The presence of two carboxylate stretches indicates the presence of two different modes of carboxylate binding.[32] The frequency of asymmetric and symmetric vibrations depends on the electronic charge density of C−O bonds and C−O bond lengths; the higher is the frequency of the asymmetric vibration, and the lower is the frequency of the symmetric vibration. Hence for compounds F_2W_4, F_4W_4, F_4W_8, and $F_{10}W_{40}$ the asymmetric vibration at 1550 cm^{-1} pertains to the symmetric vibration at 1350 cm^{-1}. Similarly, the stretches at 1600 and 1380 cm^{-1} are related. The respective experimental values are Δ_{exp} = ∼210 cm^{-1} for samples F_2W_4, F_4W_4, and F_4W_{10}, and Δ_{exp} = ∼220 cm^{-1} for the remaining samples. Both Δ_{exp} are similar and indicate the bridging chelation. However, the formation of secondary peaks indicates a different binding mode. As stated above, the carboxylate functional group has two lone pairs of electrons on each oxygen atom available for binding, the syn lone pair and the anti lone pair. It has been suggested that the syn lone pair is more basic than those in the anti position.[39] It may be possible that a syn−anti (Figure 5b) mode of binding occurs when the water ratio is increased due

ohio2/yjy-yjy/yjy-yjy/yjy99907/yjy9845d07z | xppws | 23:ver.3 | 8/6/09 | 18:56 | Msc: jp-2009-04358g | TEID: mrh00 | BATID: 00000

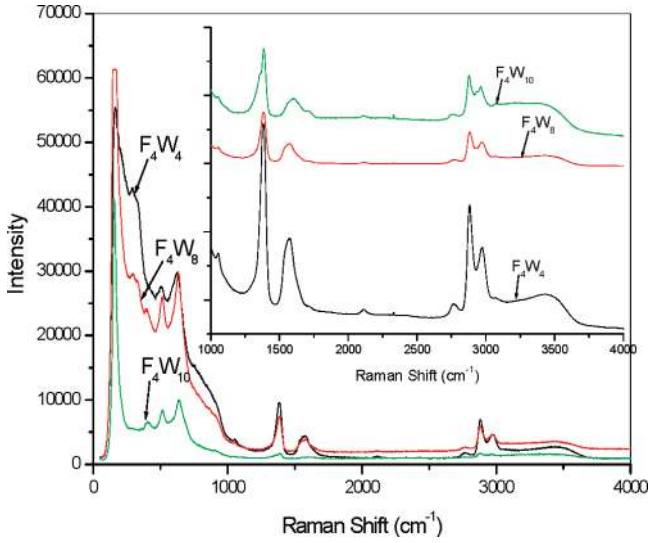

Figure 8. Raman spectra of TiO_2 precursor powders of F_4W_4−F_4W_{10}.

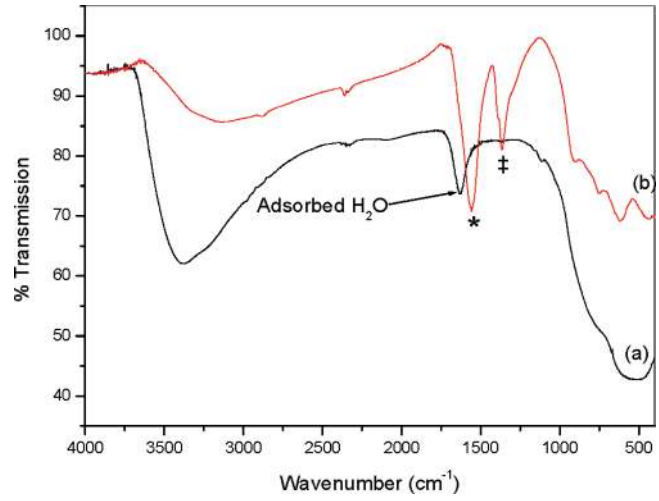

Figure 9. IR spectrum of TiO_2 precursor powders (a) $F_{control}$ and (b) F_4W_4, where * = $\upsilon_{asym}(COO^-)$ and ‡ = $\upsilon_{sym}(COO^-)$.

to the altering pH and the increased hydrolysis of the system. This would explain the appearance of secondary peaks in the IR spectra.

Zelenak et al. observed singlet peaks for both the υ_{as} and υ_s (COO^-) stretches for bridging complexes that follow syn−syn binding and they observed doublet peaks at similar wavenumbers for syn−anti binding with zinc carboxylate complexes,[32] while Ishioka et al. reported similar values of separation for syn−anti bridge in zinc(II) acetate.[50] The result of syn−anti bridging may produce a polymeric network with little branching and cross-linking that is structurally weak, therefore, forming rutile at lower calcination temperatures than that of a typical syn−syn mode of bidentate bridging.

Raman Spectroscopy. Raman spectroscopy was employed as a secondary technique to IR in order to confirm the above results.

F8 Figure 8 shows the Raman spectra of the precalcined TiO_2 powders. Although the powders have not been calcined, the Raman spectra display clear signs of the anatase phase four-peak pattern with peaks at 160, 405, 515, and 635 cm^{-1} for powders F_4W_{10}−F_4W_{100}. However, for the powders F_4W_4 and F_4W_8 (like with IR spectra) the appearance of a peak at ∼290 cm^{-1} indicates that the Ti−O structure is different than the other samples and contains a pattern similar to that of an anatase/rutile mixture. The formation of rutile-like structures during the course of crystallization of titania hydrolysate into anatase has been confirmed by several research groups.[51−53] It has been suggested that the structures which provide the anatase and rutile Raman spectral patterns disappear just before the crystallization into anatase.[53] It is apparent that the presence of the anatase/rutile-like structure for samples F_4W_4 and F_4W_8 cause an increase in the ART temperature. From Figure 8 it can also be seen that the presence of intense peaks at 1393, 1580, 2890, and 2980 cm^{-1} are only present in samples F_4W_4 and F_4W_8. In order to investigate further, all Raman spectra were repeated but scans were only carried out in the region 800−4000 cm^{-1} (the organic region) to further confirm binding modes of the formate group.

Figure 8 (inset) shows the Raman spectra of the formate group binding with the titanium. Peaks from ∼2800−3500 cm^{-1} are due to OH stretches.[33] As seen with the IR spectra, the intensity of the OH peak increases in comparison with the COO^- stretches (1392 and 1567 cm^{-1}) in F_4W_4 and F_4W_8 when compared with F_4W_{10}−F_4W_{100}. The appearance of secondary peaks also appears beside the main COO^- peaks (1392 and 1567 cm^{-1}) at 1370 and 1720 cm^{-1}. The peak at 1567 cm^{-1} is also shifted to a higher wavenumber. The formation of secondary peaks in the Raman spectra are for the same samples as those of the IR which again indicates the presence of an alternative mode of binding such as syn−anti, as was proposed previously (Figure 5).

Effect of Chelating Agent. Sample $F_{control}$ was synthesized using water only to determine what affect formic acid had on the structure of the Ti−O network both before and after calcination.

X-ray Diffraction. Without the presence of a chelating agent ($F_{control}$), rutile begins to form at a temperature as low as 600 °C (20%) and total transformation has occurred at 700 °C. Samples F_2W_{10}, F_2W_{40}, F_2W_{80}, and F_2W_{100} have a higher rutile content at 600 °C. This may be due to the chelating agent having an adverse effect on the initial TiO_2 structure whereby a syn−anti bridging mode is dominant throughout the structure thus forming a structure without cross-linking that upon calcination, forms a larger percentage of rutile at 600 °C.

Infrared Spectroscopy. In Figure 9 there is an OH stretch (2800−3600 cm^{-1}), a Ti−O stretch (400−1000 cm^{-1}), and also a signal at 1610 cm^{-1} due to the bending vibrations of adsorbed water. There is a clear difference in the IR spectra of $F_{control}$ and F_4W_4. This was expected and is due to the carboxylate group−Ti bridging structure. Also in the region 400−1000 cm^{-1}, F_4W_4 gives more defined peaks as opposed to the broad peak given by $F_{control}$. This is due to a more ordered Ti−O framework.[26,31,43]

Raman Spectroscopy. The Raman spectrum of $F_{control}$ gives no peaks of distinction. Showing that without the presence of formic acid, Ti−O atoms randomly arrange as opposed to the more ordered structure shown in Figure 8 where formic acid was employed as a chelating agent. Comparing the Raman spectra of $F_{control}$ with Figure 9, where the samples were chelated, it becomes clear that the presence of the formic acid as a chelating agent enables the metal−oxygen atoms to form a defined, crystallinelike structure which is apparent in Figure 8 (0−1000 cm^{-1}). The Raman spectra of $F_{control}$, as expected also lacks the presence of the bridging peaks present in Figure 8 at 1390 and 1570 cm^{-1}. It is the presence of this CO−Ti bridge that allows a controlled arrangement of the Ti−O atoms. Without the bridge there is uncontrolled hydrolysis leading to a random arrangement of Ti−O atoms. The Raman spectra of

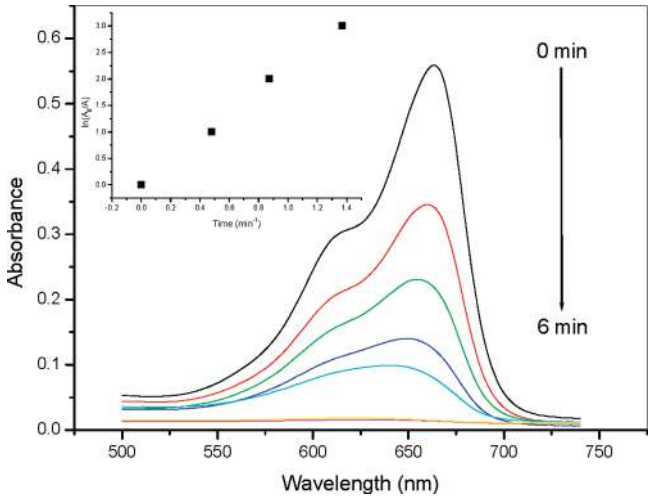

Figure 10. Photocatalytic degradation of methylene blue with F7 (700 °C).

TABLE 1: Reaction Rate Constants (±0.01, k/min^{-1}) for the Degradation of Methylene Blue

sample	600 °C	700 °C	800 °C
$F_{control}$	0.12	0.12	0.05
F_2W_4	0.17	0.20	0.17
F_4W_4	0.13	0.45	0.38
$F_{10}W_4$	0.26	0.13	0.08

$F_{control}$ compares favorably to the IR spectrum of the same sample shown in Figure 9.

Photocatalytic Studies. Photocatalytic studies were carried out on selected powders ($F_{control}$, F_2W_4, F_4W_4, and $F_{10}W_4$) at calcination temperatures (600, 700, and 800 °C) and were compared with the commercial photocatalyst, Degussa P25. Powder F_4W_4 calcined at 700 °C was found to be the most photocatalytically active (Figure 10). The methylene blue was completely degraded after 6 min.

Improved photocatalytic activity has been previously found with anatase/rutile interactions, due to improved electron−hole separation.[54−56] A mixture of both phases has given rise to the most efficient photocatalyst out of the powders synthesized. It has been suggested that an intimate contact between anatase and rutile phases may enhance the separation of photogenerated electrons and holes resulting in excellent photocatalytic efficiency.[57] It is believed that the anatase/rutile mixture present in Degussa P25 is one of the reasons why it is the one of the most investigated photocatalysts.[56] First-order degradation plots of powders $F_{control}$, F_2W_4, F_4W_4 (Figure 10 inset), and $F_{10}W_4$ at calcination temperatures 600, 700, and 800 °C were used to calculate the reaction rate constant, k (min^{-1}) (Table 1).

Sample F_4W_4 calcined at 700 °C had the largest rate constant at 0.45 min^{-1}, the rate constant for Degussa P25 was found to be 0.29 min^{-1} for the same reaction conditions. Sample F_4W_4 calcined at 700 °C consists of 87% anatase and 13% rutile to give an ideal mixture for photocatalytic efficiency for the degradation of methylene blue as a model pollutant. Sample F_2W_4 has an identical anatase/rutile mixture at 600 °C but is not as photoactive as F_4W_4. At 700 °C F_2W_4 consists of mainly rutile (72%) which results in a reduction of photocatalytic activity. At 600 and 800 °C, F_4W_4 has 0% and 32% rutile, respectively. This reduces the photocatalytic activity of F_4W_4. $F_{control}$, the sample prepared without any chelating agent was the poorest photocatalyic performer, even at 600 °C where it consisted of an anatase/rutile mixture (90:10), giving a reaction rate of 0.12 min^{-1}. As shown through IR and Raman spectroscopy, the absence of a chelating agent causes complete disorder among the Ti−O bonds upon hydrolysis resulting in an unorganized network of TiO_2 particles when compared with those where a chelating agent was present. $F_{10}W_4$ consisted of 77% rutile at 600 °C and 95% rutile at 700 °C. As reported previously,[54−57] a mixture of anatase and rutile has greater photoactivity than either phase alone. Photocatalytic studies were repeated for the same samples using rhodamine 6G as a model organic pollutant and consistent results were obtained (Supporting Information 2).

Conclusions

ART in a formic acid modified titania material has been studied using XRD, FTIR, and Raman spectroscopy. Through Raman and IR it was possible to determine the mode of binding of the chelating agent, formic acid, to the titanium precursor with the equation $\Delta = \upsilon_{as}(COO^-) - \upsilon_s(COO^-)$. A value for $\upsilon_{as}(COO^-) - \upsilon_s(COO^-)$ of 210 cm^{-1} indicated that bidentate bridging is the mode of binding for the samples. However, for samples with increased water concentrations, spectroscopy results showed doublet peaks indicating alternate modes of bridged binding. It was postulated that for these samples syn−anti binding was occurring as well as syn−syn binding. It is believed that the resulting syn−anti binding hinders cross-linking of the oligomer network, resulting in a weakened structure and thus causing the anatase to rutile transformation temperature to occur at lower temperatures than with the syn−syn mode of binding where more ordered oligomer networks are believed to be formed.

Photocatalytic studies showed that the formic acid modified sample (calcined at 700 °C) with an anatase/rutile mixture of 86:14 was more effective for the degradation of methylene blue than the commercial titania sample Degussa P25, showing that an anatase/rutile mixture is more effective than either phase alone, which is consistent with previous literature results.

Acknowledgment. The authors thank the Environmental Protection Agency for its financial support. They also thank Emer Ryan for FESEM images.

Supporting Information Available: FESEM image of calcined powders and photocatalytic testing data for rhodamine 6G. This material is available free of charge via the Internet at http://pubs.acs.org.

References and Notes

(1) Carp, O.; Huisman, C. L.; Reller, A. *Prog. Solid State Chem.* **2004**, *32*, 33.
(2) Gratzel, M. *Nature* **2001**, *414*, 338.
(3) Hoffman, M. R.; Martin, S. T.; Choi, W.; Bahnemann, D. W. *Chem. Rev.* **1995**, *95*, 69.
(4) Joung, S.-K.; Amemiya, T.; Murabayashi, M.; Itoh, K. *J. Photochem. Photobiol., A.* **2006**, *184*, 273.
(5) Skubal, L. R.; Meshkov, N. K.; Vogt, M. C. *J. Photochem. Photobiol., A.* **2002**, *148*, 103.
(6) Suresh, C.; Biju, V.; Mukundan, P.; Warrier, K. G. K. *Polyhedron* **1998**, *17*, 3131.
(7) Ye, X.; Chen, D.; Gossage, K.; Li, J. *J. Photochem. Photobiol., A.* **2006**, *183*, 35.
(8) Hu, Y.; Tsai, H.-L.; Huangk, C.-L. *Eur. Ceram. Soc.* **2003**, *23*, 691.
(9) Shao, Y.; Tang, D.; Sun, J.; Lee, Y.; Xiong, W. *China Particuol.* **2004**, *2*, 119.
(10) Aguado, J.; van Grieken, R.; Lopez-Munoz, M. J.; Marugan, J. *Catal. Today* **2002**, *75*, 95.
(11) Diebold, U. *Surf. Sci. Reports* **2003**, *48*, 53.

(12) Sim, C.-S.; Kwon, I.-M.; Moon, B. K.; Jeoung, J. H.; Choi, B. C.; Kim, J. H.; Choi, H.; Yi, S. S.; Yoo, H.; Hong, H.-S.; Park, J.-H.; Lee, H. S. **2007**, *27*, 1343.
(13) Zhang, Q.; Gao, L.; Guo, J. *Appl. Catal., B* **2000**, *26*, 207.
(14) Yoganarasimhan, S. R.; Rao, C. N. R. *Trans. Faraday Soc.* **1962**, *58*, 1579.
(15) MacKenzie, K. J. D. *Trans. J. Br. Ceram. Soc.* **1975**, *74*, 29.
(16) Byun, C.; Wang, J. W.; Kim, L. T.; Hong, K. S.; Lee, B. W. *Mater. Res. Bull.* **1997**, *32*, 431.
(17) MacKenzie, K. J. D. *Trans. J. Br. Ceram. Soc.* **1975**, *74*, 121.
(18) Li, Y.; White, T. J.; Lim, S. H. *J. Solid State Chem.* **2004**, *177*, 1372.
(19) Ding, X.-Z.; Liu, X.-H. *J. Mater. Res.* **1998**, *13*, 2556.
(20) Gribb, A. A.; Banfield, J. F. *Am. Mineral.* **1977**, *82*, 717.
(21) Zhang, H.; Banfield, J. F. *J. Mater. Chem.* **1998**, *8*, 2073.
(22) Zhang, H.; Banfield, J. F. *J. Mater. Res.* **2000**, *15*, 437.
(23) Ahn, Y. U.; Kim, E. J.; Kim, H. T.; Hahn, S. H. *Mater. Lett.* **2003**, *57*, 4660.
(24) Kumar, K. P.; Keizer, K.; Burggraaf, A. J.; Okubo, T.; Nagamoto, H. *J. Mater. Chem.* **1993**, *3*, 1151.
(25) Brinker, C. J.; Scherer, G. W. *The Physics and Chemistry of Sol−Gel Science*; Academic Press: New York, 1990.
(26) Verma, A.; Samant, S. B.; Bakhshi, A. K.; Agnihotry, S. A. *Sol. Energy Mat. Sol. Cells* **2005**, *88*, 47.
(27) Phule, P. P.; Risbud, S. H. *J. Mater. Sci.* **1990**, *25*, 1169.
(28) Takahaschi, Y.; Matsuoka, Y. *J. Mater. Sci.* **1988**, *23*, 2259.
(29) Takahaschi, Y.; Kiwa, K.; Kobayashi, K.; Matsuki, M. *J. Am. Ceram. Soc.* **1991**, *74*, 67.
(30) Sanchez, C.; Livage, J.; Henry, M.; Babonneau, F. *J. Non-Cryst. Solids* **1988**, *100*, 65.
(31) Guilment, J.; Pencelot, O.; Rigola, J.; Truchet, S. *Vib. Spectrosc.* **1996**, *11*, 37.
(32) Zelenak, V.; Vargova, Z.; Gyoryova, K. *Spectrochim. Acta* **2007**, *66*, 262.
(33) Nakamoto, K. *Infrared and Raman Spectra of Inorganic and Coordinated Compounds, Part B*; John Wiley: New York, 1997.
(34) Nara, M.; Tasumi, M.; Tanokura, M.; Hiraoki, T.; Yazawa, M.; Tsutsumi, A. *FEBS Lett.* **1994**, *349*, 84.
(35) Czakis-Sulikowska, D.; Czylkowska, A.; Malinowska, A. *J. Therm. Anal. Cal.* **2002**, *67*, 667.
(36) Deacon, G. B.; Phillip, R. J. *Coord. Chem. Rev.* **1980**, *33*, 227.
(37) Lewandowski, W.; Fuks, L.; Lewandowski, H. *J. Inorg. Biochem.* **2005**, *99*, 1407.
(38) Manhas, B. S.; Trikha, A. K. *J. Indian Chem. Soc.* **1982**, *59*, 315.
(39) Rardin, R. L.; Tolman, W. B.; Lippard, S. J. *New. J. Chem.* **1991**, *15*, 417.
(40) Pillai, S. C.; Periyat, P.; George, R.; McCormack, D. E.; Seery, M. K.; Hayden, H.; Colreavy, J.; Corr, D.; Hinder, S. J. *J. Phys. Chem. C* **2007**, *111*, 1605.
(41) Guillard, C.; Beaugiraud, B.; Dutriez, C.; Herrmann, J.-M.; Jaffrezic, H.; Jaffrezic-Renault, N.; Lacroix, M. *Appl. Catal., B* **2002**, *39*, 331.
(42) Nguyen, T.-V.; Choi, D.-J.; Yang, O.-B. *Res. Chem. Intermed.* **2005**, *31*, 483.
(43) Ivanda, M.; Music, S.; Popovic, S.; Gotic, M. *J. Mol. Struct.* **1999**, *480−481*, 645.
(44) Spurr, R.; Myers, H. *Anal. Chem.* **1957**, *29*, 760.
(45) Q-Sun. Vol. 2009; p Q.
(46) Urlaub, R.; Posset, U.; Thull, R. *J. Non-Cryst. Solids* **2000**, *265*, 276.
(47) Kung, H. H.; Ko, E. I. *Chem. Eng. J.* **1996**, *64*, 203.
(48) Sahni, S.; Bhaskar Reddy, S.; Murty, B. S. *Mater. Sci. Eng.* **2007**, *452−453*, 758.
(49) Livage, J.; Sanchez, C.; Henry, M.; Doeuff, S. *Solid State Ionics* **1989**, *32/33*, 633.
(50) Ishioka, T.; Shibata, Y.; Takahaski, M.; Kaneska, I.; Kitagawa, Y.; Nakamura, K. T. *Spectrochim. Acta, Part A* **1998**, *54*, 1827.
(51) Hwang, D. S.; Lee, N. H.; Lee, D. Y.; Song, J. S.; Shin, S. H.; Kim, S. J. *Smart Mat. Struct.* **2006**, *15*, S74.
(52) Kittaka, S.; K., M.; Takahara, S. *J. Solid State Chem.* **1997**, *132*, 447.
(53) Yoshitake, H.; Abe, D. *Microporous Mesoporous Mater.* **2009**, *119*, 267.
(54) Bickley, R. I.; Gonzalez-Carreno, T.; Lees, J. S.; Palmisano, L.; Tilley, R. J. D. *J. Solid State Chem.* **1991**, *92*, 178.
(55) Hurum, D. C.; Agrios, A. G.; Gray, K. A.; Rajh, T.; Thurnauer, M. C. *J. Phys. Chem. B* **2003**, *107*, 4545.
(56) Yu, J.; Yu, H.; Cheng, B.; Zhou, M.; Zhao, X. *J. Mol. Catal. A: Chem.* **2006**, *253*, 112.
(57) Datye, A. K.; Riegel, G.; Bolton, J. R.; Huang, M.; Prairie, M. R. *J. Solid State Chem.* **1995**, *115*, 236.

JP904358G